

Synthesis and Assembly of Self-Complementary CavitanDs

Adam R. Renslo, Fabio C. Tucci, Dmitry M. Rudkevich, and Julius Rebek, Jr.*

Contribution from The Skaggs Institute for Chemical Biology and the Department of Chemistry, The Scripps Research Institute, 10550 North Torrey Pines Rd., La Jolla, California 92037

Received November 5, 1999

Abstract: CavitanDs with self-complementary shapes (**3** and **4**) were prepared by the covalent attachment of adamantane guest molecules to the upper rim of the host structures. Relatives of the “self-folding” cavitanDs **2**, these new structures possess a seam of intramolecular hydrogen bonds that stabilize the folded conformation. Their self-complementary shapes result in the formation of noncovalent dimers of considerable kinetic and thermodynamic stability ($-\Delta G^{295} = 4.5$ kcal/mol for **3a** and 6.5 kcal/mol for **4a** in *p*-xylene-*d*₁₀). The dimerization of cavitanDs **3** and **4** is reversible and subject to control by solvent and temperature. The dimerization process is enthalpically favored and entropy opposed and occurs with significant enthalpy–entropy compensation.

Introduction

Small molecule guests can be surrounded by larger host structures either reversibly or irreversibly. Within the host–guest complex molecular recognition is expressed and it has consequences for both host and guest: molecular surfaces in contact with each other are protected from solvent and reagents in the bulk solution, and complexation increases the components' stabilities.¹ While the complex exists it may also express new forms of stereochemistry² and stereoselectivity,³ reactive intermediates can be generated with protracted lifetimes,⁴ and even catalysis of reactions can take place.⁵ If the reaction involves covalent bonding between host and guest, a self-complementary structure results, and the new molecule may catalyze its own formation: it may replicate.⁶ Complementarity of the host and guest is the germ of these possibilities and we examine here hosts and guests of the most primitive sort of shape complementarity: concave with convex.

CavitanDs—molecular cavities with one open end—are among the simplest of concave molecules and they hold a prominent place in the history of synthetic host structures.⁷ Specifically, the resorcinarenes **1** (Scheme 1) present a bowl-shaped inner surface and are accessible by Högborg's⁸ high-yielding condensation of resorcinol with various aldehydes. These were used

directly as hosts by Aoyama⁹ and modified by Cram,¹⁰ to become modules for the construction of carcerands¹¹ and velcrands.¹² The latter work established the conformational preferences and interconversion dynamics of the resorcinarene-derived cavitanDs as subject to control by temperature and solvent. Subsequently, we installed a hydrogen-bonded seam along the upper rim of the structure, to hold the conformation in the vase-like shape shown as in **2**. This gave rise to “self-folding” cavitanDs.¹³

Appropriately convex guest molecules for these cavitanD hosts were found in adamantane derivatives. The complementarity of size is obvious from modeling but the complementarity of shape is not. The cavitanD has a 4-fold axis of symmetry while the 1-substituted adamantanes have a 3-fold axis. But most space-filling renderings of adamantane show it to be nearly spherical whereas the appropriate cross section of the host is nearly circular. Somewhat less obvious is the complementarity of chemical surfaces. Almost all the atoms that line the cavity are sp² hybridized with their p orbitals directed inward, so the concave surface may be thought to present a thin layer of negative charge. For sp³ hybridized C–H bonds this environment offers little intrinsic appeal although a multitude of attractions can be hidden within C–H/π interactions, van der Waals forces, and solvophobicity. Cyclohexanes were also welcome guests, even though their shapes were less complementary to the host. Cubane would seem ideal since its C–H bonds of higher s character present a thin layer of positive charge

(1) (a) Cram, D. J.; Cram, J. M. *Container Molecules and Their Guests*; Royal Society of Chemistry: Cambridge, 1994. (b) Conn, M. M.; Rebek, J., Jr. *Chem. Rev.* **1997**, *97*, 1647. (c) Rebek, J., Jr. *Acc. Chem. Res.* **1999**, *32*, 278–286.

(2) van Wageningen, A. M. A.; Timmerman, P.; van Duynhoven, J. P. M.; Verboom, W.; van Veggel, F. C. J. M.; Reinhoudt, D. N. *Chem. Eur. J.* **1997**, *3*, 639–654.

(3) Rivera, J. M.; Martín, T.; Rebek, J., Jr. *Science* **1998**, *279*, 1021–1023.

(4) (a) Cram, D. J.; Tanner, M. E.; Thomas, R. *Angew. Chem., Int. Ed. Engl.* **1991**, *30*, 1024–1027. (b) Warmuth, R. *Angew. Chem., Int. Ed. Engl.* **1997**, *36*, 1347–1350. (c) Beno, B. R.; Sheu, C.; Houk, K. N.; Warmuth, R.; Cram, D. J. *Chem. Commun.* **1998**, 301–302.

(5) Kang, J.; Santamaria, J.; Hilmersson, G.; Rebek, J., Jr. *J. Am. Chem. Soc.* **1998**, *120*, 7389–7390.

(6) Wintner, E. A.; Conn, M. M.; Rebek, J., Jr. *Acc. Chem. Res.* **1994**, *27*, 198–203.

(7) (a) Cram, D. J. *Science* **1983**, *219*, 1177–1183. (b) Rudkevich, D. M.; Rebek, J., Jr. *Eur. J. Org. Chem.* **1999**, *64*, 1991–2005.

(8) (a) Högborg, A. G. S. *J. Am. Chem. Soc.* **1980**, *102*, 6046–6050. (b) Högborg, A. G. S. *J. Org. Chem.* **1980**, *45*, 4498–4500.

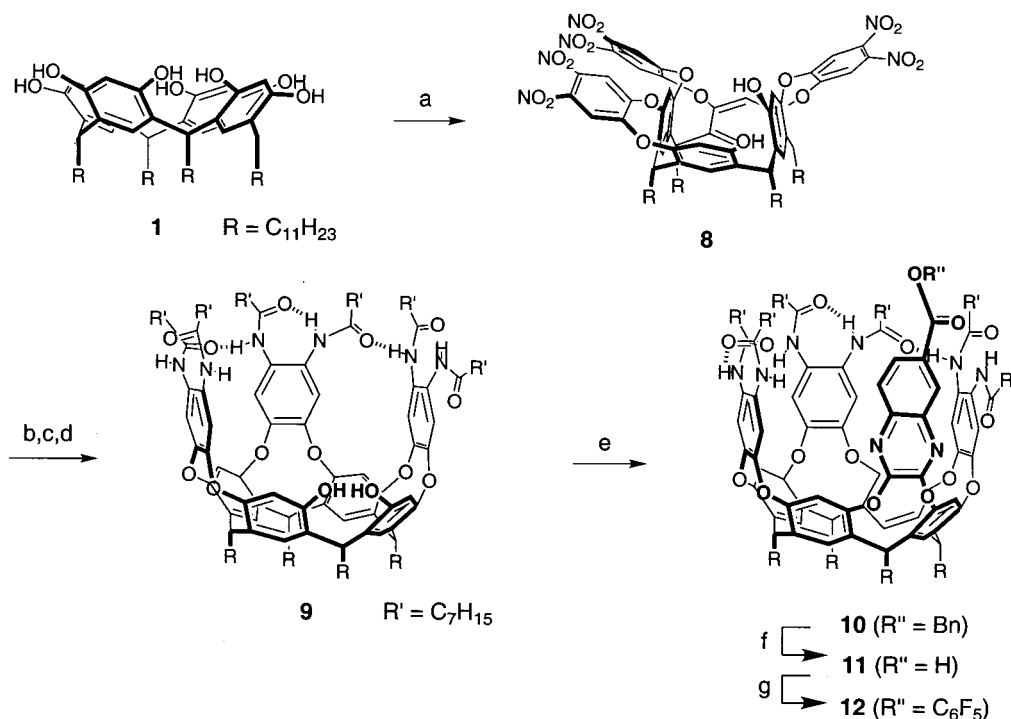
(9) (a) Kikuchi, Y.; Kato, Y.; Tanaka, Y.; Toi, H.; Aoyama, Y. *J. Am. Chem. Soc.* **1991**, *113*, 1349–1354. (b) Kobayashi, K.; Asakawa, Y.; Kikuchi, Y.; Toi, H.; Aoyama, Y. *J. Am. Chem. Soc.* **1993**, *115*, 2648–2654.

(10) (a) Moran, J. R.; Karbach, S.; Cram, D. J. *J. Am. Chem. Soc.* **1982**, *104*, 5826. (b) Cram, D. J.; Karbach, S.; Kim, H.-E.; Knobler, C. B.; Maverick, E. F.; Ericson, J. L.; Helgeson, R. C. *J. Am. Chem. Soc.* **1988**, *110*, 2229. (c) Reference 1a, pp 85–130.

(11) For reviews, see: (a) Jasat, A.; Sherman, J. C. *Chem. Rev.* **1999**, *99*, 931–967. (b) Reference 1a, pp 131–216.

(12) (a) Moran, J. R.; Ericson, J. L.; Dalcanale, E.; Bryant, J. A.; Knobler, C. B.; Cram, D. J. *J. Am. Chem. Soc.* **1991**, *113*, 5707–5714. (b) Cram, D. J.; Choi, H.-J.; Bryant, J. A.; Knobler, C. B. *J. Am. Chem. Soc.* **1992**, *114*, 7748–7765.

(13) (a) Rudkevich, D. M.; Hilmersson, G.; Rebek, J., Jr. *J. Am. Chem. Soc.* **1997**, *119*, 9911–9912. (b) Rudkevich, D. M.; Hilmersson, G.; Rebek, J., Jr. *J. Am. Chem. Soc.* **1998**, *120*, 12216–12225. (c) Ma, S.; Rudkevich, D. M.; Rebek, J., Jr. *Angew. Chem., Int. Ed. Engl.* **1999**, *38*, 2600–2602.

Scheme 1^a

^a Conditions: (a) 3.0 equiv of 1,2-difluoro-4,5-dinitrobenzene, 12 equiv of Et_3N , DMF, 70 °C, 18 h, (45–56%); (b) H_2 , $RaNi$, toluene, 40 °C, 15 h; (c) 6 equiv of $C_7H_{15}COCl$, 12 equiv of K_2CO_3 , $EtOAc-H_2O$; (d) 10 equiv of $H_2NNH_2-H_2O$, $EtOH$ -toluene, reflux, 3 h, (25–30% overall from **8**); (e) 1.1 equiv of **14**, DMF, 6.0 equiv of Et_3N , 85 °C, 2 d, 55%; (f) H_2 , Pd/C , $EtOAc$, room temperature, 2 h; (g) 1.2 equiv of C_6F_5OH , 2.0 equiv of $EDC-MeI$, cat. DMAP, THF, room temperature, 20 h, 80% from **10**.

on the surface, with shape complementarity to boot. Indeed cubane proved an excellent guest for the related calixarene capsules, but simple substituted derivatives are much less available for screening than adamantanes or cyclohexanes. The most appropriate complements—molecules with a thin layer of positive charge—were found in quinuclidinium salts, and we have made much use of these as guests for characterization of complexes in the gas phase by electrospray mass spectrometry.¹⁴ These guests lack sufficient solubility for the solution studies contemplated here.

Finally, the hydrogen bonding characteristics of the guest's functions also contribute to binding. Substituents that feature hydrogen bond donors or acceptors can interact with the seam of amides that hold the host together; substituents that feature both, such as secondary amides, are especially welcome.¹³ The sum of these recognition forces is modest; typically ≤ 2 kcal/mol in binding affinity is observed for complexation in organic solvents; their thermodynamic stability is low. What makes these systems special is their unprecedented *kinetic* stability. The energetic barriers for exchange of guests in and out of the cavities are among the highest observed for open-ended vessels.^{7b} For example, adamantane exchange in xylene occurs with a free energy of activation, ΔG^\ddagger of 17 kcal/mol.^{13a} Accordingly, the rate is slow on the NMR time scale (600 MHz, ambient temperatures) and separate signals are observed for free species and the complexes. The resonances of the complexed guests appear far upfield, between 0 and -3 ppm. This open window of the spectra allows easy determination of concentrations, from which equilibrium constants and thermodynamic parameters can be calculated. The lifetimes of the complexes are long enough to expect that many types of reaction processes could occur between host and guest.

The self-complementary cavitannds (**3** and **4**) (Chart 1) described here are cousins of cavitannd **2** to which adamantane guests were covalently attached on their upper rims. The resulting structures could, from their self-complementarity, form cyclic oligomers of any size or even polymerize, but they form dimers in solution. The cooperative nature of the process gives high thermodynamic and kinetic stability to the dimeric complexes.

These are not the first self-including cavitannd dimers. Efforts directed at the deepening of cavitannds to accommodate increasingly larger guests earlier produced two other examples. The tetraester **6** prepared by Cram¹⁵ and co-workers formed a dimeric species (Chart 2) in the solid state and in solution at high concentrations (50 mM). Likewise, the tetraamide **7** forms a hydrogen bonded dimer in which one upper-rim alkyl chain from each monomer is bound within the cavity of the dimer.¹⁶ The SCCs described here were engineered to maximize the efficacy of a self-complementary binding motif. We now provide a full account of our studies directed at the synthesis and assembly of these self-complementary molecules.¹⁷

Results and Discussion

Synthesis. The synthesis of cavitannds featuring a unique site required the selective tri-arylation¹⁸ of Högberg's resorcinarene **1**. This was accomplished as illustrated in Scheme 1. Reaction of the resorcinarene **1** with 3 equiv of 1,2-difluoro-4,5-dinitro-

(15) von dem Bussche-Hünnefeld, C.; Helgeson, R. C.; Böhning, D.; Knobler, C. B.; Cram, D. J. *Croat. Chem. Acta* **1996**, *69*, 447–458.

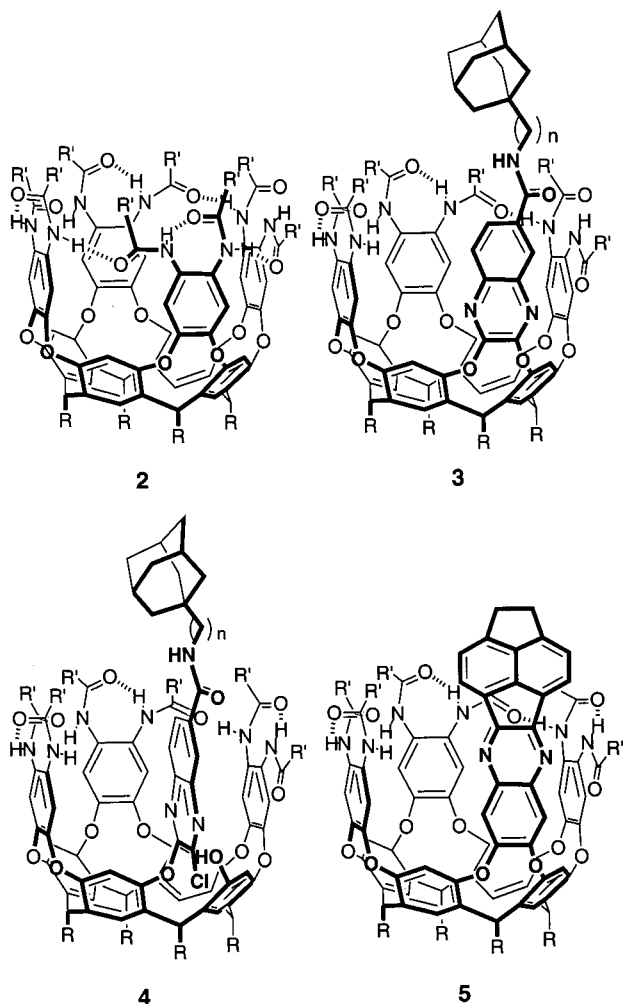
(16) Ma, S.; Rudkevich, D. M.; Rebek, J., Jr. *J. Am. Chem. Soc.* **1998**, *120*, 4977–4981.

(17) For the preliminary communication see: Renslo, A. R.; Rudkevich, D. M.; Rebek, J., Jr. *J. Am. Chem. Soc.* **1999**, *121*, 7459–7460.

(18) Selective tri-arylation of a resorcinarene with quinoxaline dichlorides was reported previously, see: (a) Soncini, P.; Bonsignore, S.; Dalcaneale, E.; Uguzzoli, F. *J. Org. Chem.* **1992**, *57*, 4608–4612. (b) Reference 10a.

(14) Schalley, C. A.; Castellano, R. K.; Brody, M. S.; Rudkevich, D. M.; Siuzdak, G.; Rebek, J., Jr. *J. Am. Chem. Soc.* **1999**, *121*, 4568–4579.

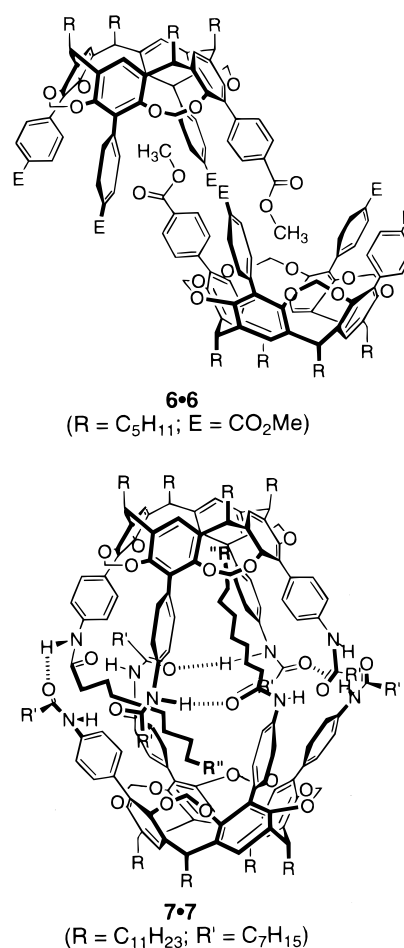
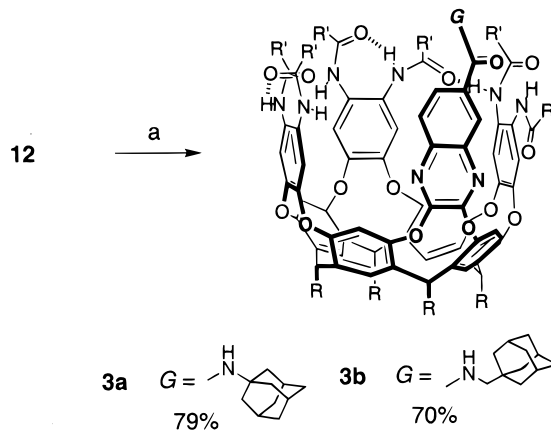
Chart 1



benzene in DMF/Et₃N produced the desired hexanitro cavitand **8** (45–56%) which exists in equilibrium between the “kite” and “vase” conformations. A smaller quantity (<20%) of the fully bridged, octanitro compound is also formed but could be easily separated from **8** by column chromatography. Installation of the upper-rim seam of head-to-tail amides was initiated by reduction of the hexanitro compound with Raney Ni and H₂ in toluene. The resulting hexaamino cavitand was immediately acylated with octanoyl chloride under Schotten–Baumann conditions (K₂CO₃, EtOAc–H₂O). The free phenolic groups were acylated simultaneously, but the resulting esters were cleaved by brief treatment with H₂NNH₂ in toluene–EtOH. This provided the hexaamide cavitand **9** (R' = C₇H₁₅) in 25–30% overall yield from the hexanitro cavitand **8**. Although the hydrogen-bonded seam in hexaamide **9** is incomplete, the cavitand still adopts the desired folded conformation in solution as evidenced by NMR (vide infra).

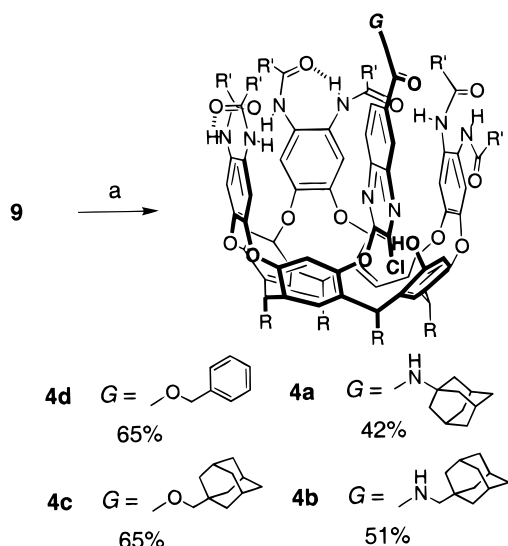
At this juncture, the syntheses of cavitaids **3** and **4** diverge. The SCCs **3** are most conveniently and reliably prepared from the activated ester **12** (Scheme 1). Hence, coupling of the quinoxaline dichloride **14** with hexaamide **9** in DMF at 85 °C produces the desired benzyl ester **10** in 55% yield. Hydrogenolysis of **10** (H₂, Pd/C) and activation of the resulting acid **11** (C₆F₅OH, EDC–MeI, cat. DMAP, THF) provides the pentafluorophenyl ester **12** in 80% overall yield. This activated ester is then employed in the synthesis of SCCs **3a** and **3b** by reaction with adamantane nucleophiles (1-amino or 1-amino-methyl) under mild conditions (DMF or CH₂Cl₂ at room

Chart 2

Scheme 2^a

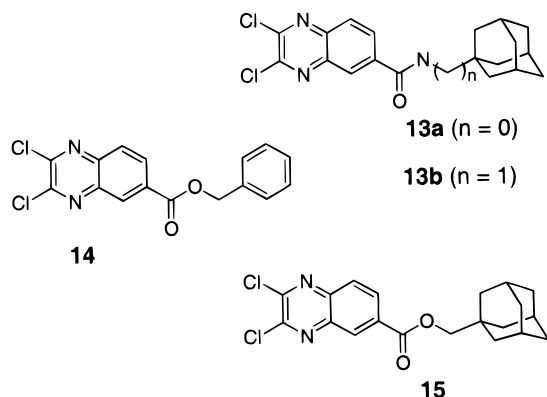
^a Conditions: (a) 1.3 equiv of 1-aminoadamantane, 4.0 equiv of Et₃N, DMF, room temperature, 16h (79% **3a**) or 1.3 equiv of 1-methylaminoadamantane, 4.0 equiv of Et₃N, CH₂Cl₂, room temperature, 24 h (70% **3b**).

temperature, Scheme 2). The formation of cavitaids **4** in which only one position on the quinoxaline heterocycle has undergone reaction was unexpected and is, to the best of our knowledge, without literature precedent. It took us sufficiently by surprise that we mis-assigned their structures in our recent communication¹⁷ and here we correct them. To be sure, reaction of hexaamide **9** with quinoxalines **13**–**15** under standard coupling conditions (DMF–Et₃N, 65 °C), as in Scheme 3, gives SCCs **3** as reported. It is, however, the minor product and not the one

Scheme 3^a

^a Conditions: (a) 1.1 equiv of quinoxaline **13**–**15**, 6.0 equiv of Et₃N, DMF, 65 °C, 20–40 h.

whose NMR spectra were published. Those spectra correspond to the major products, the “half-bridged” cavitands **4**.¹⁹ The misassignment was discovered only through the independent synthesis of **3** via the activated ester **12**, as outlined in Scheme 2. The use of more forcing reaction conditions did not lead to



a significant increase in the proportion of the fully bridged SCCs **3** except in reactions with the benzyl ester-substituted quinoxaline **14**. These results may reflect conformational constraints that prevent the nucleophilic and electrophilic sites in SCCs **4a** and **4b** from reacting to form the fully bridged systems.²⁰ Fortunately, the dimerization behavior of fully bridged and partially bridged SCCs is a matter of degree rather than kind.

A second approach to the synthetic elaboration of **9** is illustrated in Scheme 4 for the synthesis of the model compound **5**. This cavitand lacks a complete hydrogen-bonding seam and bears a large acenaphthene surface in lieu of the quinoxalines of **3** and **4**. Hence, reaction of the hexaamide **9** with 1,2-difluoro-4,5-dinitrobenzene (DMF–Et₃N, 70 °C) provided the corresponding dinitro cavitand (**16**) which upon reduction of the nitro

(19) A single regioisomer is formed. We presume that nucleophilic attack occurs at the more electrophilic position on quinoxaline dichlorides to give the regioisomer shown (i.e., SCCs **4**).

(20) Dalcanale and Cram report the successful coupling of an *unactivated* quinoxaline dichloride with a trisubstituted quinoxaline cavitand (see ref 18). The partial coupling we observe might be a consequence of the additional functionality present in our partially substituted cavitand (i.e., the C₇H₁₅ amide groups around the upper rim of the structure).

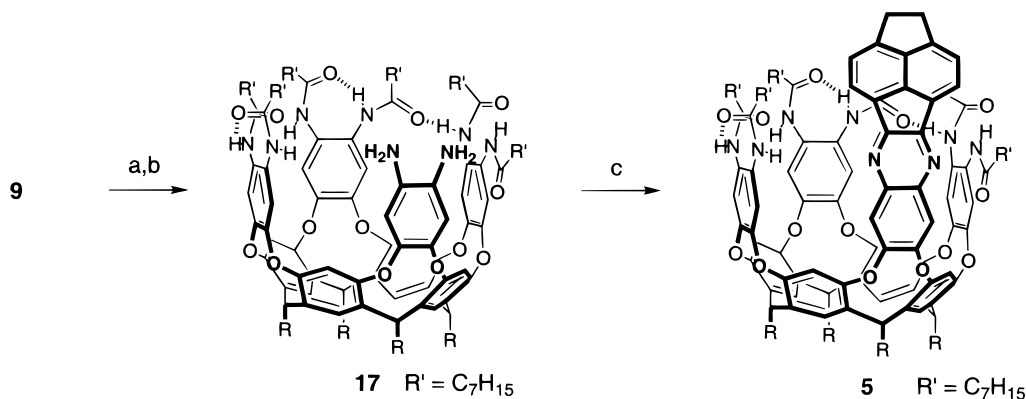
functions (H₂, RaNi, toluene) produced the diamine **17**. Condensation of this diamine with 1,2-diketopyracene produced cavitand **5**.

Complexation in Open Containers. The octaamide **2** has been characterized in detail¹³ and, as mentioned above, adamantane or cyclohexane derivatives and some lactams are bound with association constants generally ≤ 200 M⁻¹. In the present study, we investigated the thermodynamics of binding in octaamide cavitand **2** and also cavitand **5** using *N*-(1-adamantyl)acetamide as guest in *p*-xylene-*d*₁₀ and toluene-*d*₈ solvent,²¹ respectively. Although cavitand **5** lacks a complete hydrogen bonding seam (as in **2**), guest exchange remains slow on the NMR time scale. Variable temperature NMR was used to determine equilibrium constants and van't Hoff plots provided the following thermodynamic parameters. Guest binding in **2** and **5** is weak ($\Delta G^{295} = -2.2$ kcal/mol and $\Delta G^{270} = -1.5$ kcal/mol, respectively) and enthalpically driven and entropy opposed ($\Delta H = -5.5$ and -2.1 kcal/mol; $\Delta S = -11$ and -2.2 eu, respectively). The favorable binding enthalpy for **2** and **5** is attributed to van der Waals and CH– π contacts between the aromatic walls of the cavity and the aliphatic guests, and some hydrogen bonding interactions where possible. The entropy of binding in **2** is unexceptional for bimolecular host–guest complexation in organic solvents. For **5** both the enthalpy and entropy are unusually small. Since the same guest is involved and the complexes are expected to be similar in structure, the peculiarity of **5** must arise from its resting (ground) state in the toluene solvent.

The spectroscopic properties and complexation behavior of the partially substituted hexaamide cavitand **9** were also examined. Compared to **2**, hexaamide **9** lacks both a complete hydrogen bonding seam and also one of the four aromatic residues that make up the cavitand “walls”. Downfield signals in the ¹H NMR spectrum of hexaamide **9** and an N–H stretching band at 3234 cm⁻¹ (FTIR) indicate the formation of upper-rim hydrogen bonding. At the same time, the presence of methine signals at 6.2 (3 H) and 4.7 ppm (1 H) is characteristic of a fully folded “vase”¹² conformation. Accordingly, the presence of *four* aromatic “walls” and a complete seam of hydrogen bonds (as in octaamide **2**) is *not a prerequisite of the folded conformation*. Most surprisingly, the partially formed cavity in hexaamide **9** binds guest molecules with an affinity comparable to the cavity in octaamide **2** (Figure 1). Association constants of $K_{\text{ass}} = \sim 40$ and ~ 60 M⁻¹ (295 K, *p*-xylene-*d*₁₀) were calculated for the binding of *N*-(1-adamantyl)acetamide in octaamide **2** and hexaamide **9**, respectively. A broadening of signals for guests bound in hexaamide **9** (Figure 1B) probably reflects a higher exchange rate constant, but exchange remains slow on the NMR time scale at room temperature!

Characterization. Self-complementary cavitands **3** and **4** were characterized by ¹H NMR, FTIR, and MALDI-TOF spectrometry. The FTIR spectra of **3** and **4** in CHCl₃ show hydrogen-bonded N–H signals at 3238–3245 cm⁻¹ and less intense signals for free N–H stretching at 3407–3416 cm⁻¹. Figure 2 shows portions of the ¹H NMR spectra of SCC **3a** in CDCl₃, benzene-*d*₆, and *p*-xylene-*d*₁₀ solution. In CDCl₃ (Figure 2A), three hydrogen-bonded N–H signals (out of six) are observed downfield of 9.5 ppm while in *p*-xylene-*d*₁₀ solution (Figure 2C) five of the six N–H signals are located in this position. In both solvents, one amide N–H is not hydrogen bonded and its resonance appears upfield near 6 ppm. The

(21) The weak binding of guests in cavitand **5** required study at temperatures below the melting point of *p*-xylene-*d*₁₀ and so toluene-*d*₈ solvent was used with **5**.

Scheme 4^a

^a Conditions: (a) 2.0 equiv of 1,2-difluoro-4,5-dinitrobenzene, 10 equiv of Et₃N, DMF, 70 °C, 14 h (70–85% for **16**); (b) H₂, RaNi, toluene, 40 °C, 3 h, (65% for **17**); (c) 3.0 equiv of 1,2-diketopyracene, THF–AcOH, reflux, 12–16 h, (50% for **5**).

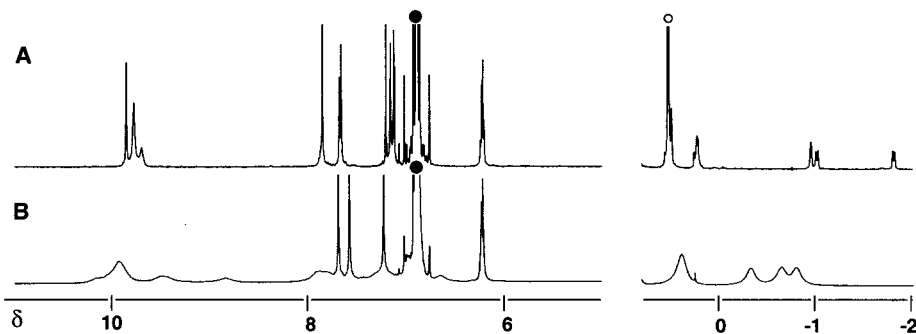


Figure 1. Portions of the ¹H NMR spectra (600 MHz, *p*-xylene-*d*₁₀, 295 K) of *N*-(1-adamantyl)acetamide in the presence of cavitannd **2** (A) and cavitannd **9** (B). Signals for residual protonated solvent and other solvent impurities are indicated by filled and open circles, respectively.

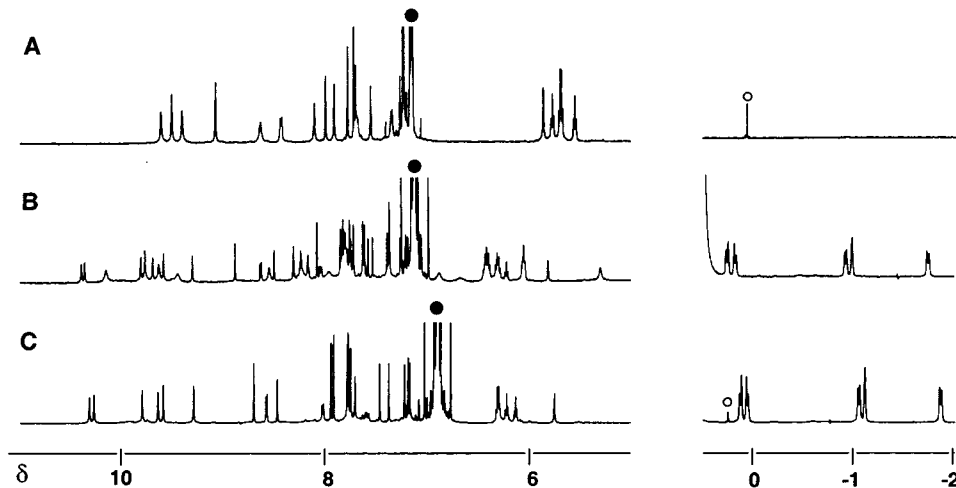


Figure 2. Portions of the ¹H NMR spectra (600 MHz, 295 K) of cavitannd **3a** in CDCl₃ (A), benzene-*d*₆ (B), and *p*-xylene-*d*₁₀ (C). Solvent peaks are denoted as before.

spectrum of **3a** is considerably more complex in benzene-*d*₆ (Figure 2B) than in CDCl₃ or *p*-xylene-*d*₁₀, and close inspection reveals the presence of two species in roughly equal quantities. The methine signals of the cavitannd are located near 6 ppm in all three solvents, as expected for the folded conformation. The most striking difference between the spectra is found in the far upfield region between 0 and –2 ppm. Whereas no upfield signals are observed in CDCl₃, in benzene-*d*₆ and *p*-xylene-*d*₁₀ a full set of adamantane signals are present. ¹H NMR spectra of the homologous SCC **3b** are similar to those of **3a**: both possess downfield N–H resonances and upfield adamantane signals (in *p*-xylene-*d*₁₀ and benzene-*d*₆ but not in CDCl₃). The ¹H NMR spectrum of **3b** in *p*-xylene-*d*₁₀ is significantly more

complex than that of **3a** in the same solvent whereas in CDCl₃ both SCCs show relatively simple and similar resonances.

Figure 3 presents the ¹H NMR spectra of the half-bridged SCCs **4a** (Figure 3A) and **4b** (Figure 3B) in *p*-xylene-*d*₁₀ solution published earlier as **3a** and **3b**. Methine signals near 6 ppm are indicative of the folded “vase” conformation. The aromatic and far downfield portions of the spectra are similar and, as with SCCs **3**, both spectra feature adamantane signals in the upfield window. The adamantane and cavitannd signals in **4b** are more complex than are those in **4a**, much as the spectrum for **3b** is more complex than that of **3a**. Compared to fully bridged SCC **3a**, the adamantane signals in **4a** are shifted downfield by ~0.5–0.7 ppm (compare C in Figure 2 and A in

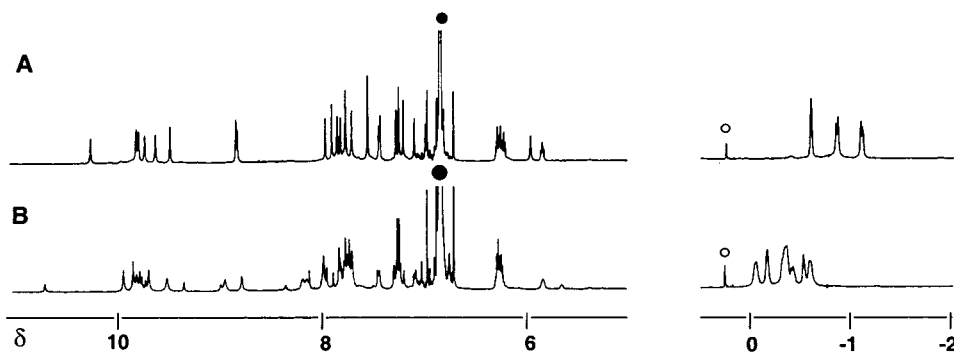


Figure 3. Portions of the ^1H NMR spectra (600 MHz, *p*-xylene- d_{10} , 295 K) of cavitands **4a** (A) and **4b** (B). Solvent peaks are denoted as before.

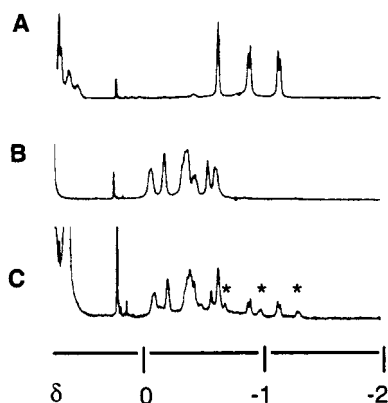


Figure 4. Upfield region of the ^1H NMR spectra (600 MHz, *p*-xylene- d_{10} , 295 K) of cavitands **4a** (A), **4b** (B), and a mixture of **4a** and **4b** (C). Signals attributed to cavitand **4a** in heterodimer **4a**·**4b** are denoted with asterisks.

Figure 3). When two different SCCs (**4a** and **4b**) were mixed in *p*-xylene- d_{10} and an NMR spectrum was recorded, a new set of bound adamantane signals appeared along with the original signals for **4a** and **4b** (Figure 4).

Discussion

The NMR and FTIR data for SCCs **3** and **4** confirm the presence of hydrogen bonding along the upper rim of the structures. The data also suggest stronger hydrogen bonding in less competitive solvents such as *p*-xylene- d_{10} and somewhat weaker hydrogen bonding in CDCl_3 . The observed chemical shifts of the methine protons provide further evidence in support of the desired “vase” conformation, as does the presence of adamantane signals in the far upfield window. This evidence of adamantane inclusion is strongly suggestive of dimerization both from an entropic standpoint and from the inspection of molecular models. The possibility of intramolecular self-inclusion can be discounted because the tether between cavity and adamantane is simply too short. Models of higher-order assemblies reveal significant conformational constraints on the upper-rim amide substituents ($\text{R}' = \text{C}_7\text{H}_{15}$). Minimized structures of dimeric species (Figures 6 and 7) reveal less significant conformational constraints. Integration of the signals for bound adamantane and total methine protons allowed the determination of a dimerization constant (K_{dim}). In the case of SCC **3a**, a value of $K_{\text{dim}} = 3000 \text{ M}^{-1}$ was calculated. This value is roughly the square of that for the binding of adamantane guests in open-ended cavitands such as **2** ($K_{\text{ass}} = \sim 40 \text{ M}^{-1}$). The stronger binding observed in SCCs is likely a consequence of their self-complementary shape and a corresponding cooperative action of binding sites.

^1H NMR data for the half-bridged SCCs **4** suggest that they too form strong assemblies in noncompetitive solvents. This is perhaps not surprising since these cavitands also possess self-complementary shapes. The significantly different chemical shifts observed for bound adamantane in SCCs **3** and **4** suggest a structurally distinct binding cavity in the two classes of SCCs. The fully formed cavity in SCCs **3** provides a more shielded microenvironment for adamantane and its signals are shifted further upfield. The more exposed cavity of the half-bridged SCCs **4** is less shielding and the corresponding upfield shift is smaller in magnitude. This analysis is undoubtedly an oversimplification since the specific orientation of adamantane in the binding cavity is also important and may well contribute to the different chemical shifts observed in these two families of SCCs. Indeed, the adamantane signals observed for half-bridged cavitands **4a** and **4b** are quite different, the signals in **4b** being less well separated and shifted less upfield (Figure 3). Since the cavities in **4a** and **4b** are identical, adamantane orientation within the cavity must be quite different in the two dimers, thus producing the dissimilar signals observed by NMR spectroscopy.

The half-bridged SCCs **4** form significantly stronger assemblies than their fully bridged brethren. In *p*-xylene- d_{10} at mM concentrations, only dimeric species are observed for SCCs **4a** and **4b**, suggesting dimerization constants $K_{\text{dim}} \geq 10^5 \text{ M}^{-1}$. In contrast to SCCs **3**, significant dimerization of half-bridged SCCs **4** is observed in CDCl_3 , a solvent that competes well for the cavity. Molecular modeling provides a possible explanation for the increased affinity. The single-bond connectivity between cavity and quinoxaline ring in SCCs **4** allows for the formation of a more extended dimeric structure (Figure 7) in which the upper-rim amide substituents are completely free of conformational constraints. This more open structure also permits favorable aromatic stacking interactions between the quinoxaline rings of the dimer.

The unsymmetrical quinoxaline wall in SCCs **3** and **4** renders the cavitands inherently chiral. The presence of a directional hydrogen bonding seam (clockwise or counterclockwise) is expected to result in conformational diastereomers. However, NMR spectra of **3a** and **4a** (Figures 2 and 3) reveal only six amide NH resonances, suggesting that the chirality of the cavitand leads to a preference for one of the two possible cyclodiastereomers. Rapid interconversion of cyclodiastereomers seems a less likely explanation considering the nonpolar solvents employed and our experience with octaamide **2** (in which the interconversion is slow on the NMR time scale).

Even assuming a preference for one monomeric cyclodiastereomer, the assembly process itself is expected to involve the formation of two diastereomeric dimers—as enantiomer pairs (denoted here “*R*·*R/S*·*S*” and “*R*·*S/S*·*R*”). Modeling the “*R*·*R/S*·*S*” diastereomer reveals a C_2 rotational axis of symmetry whereas the “*R*·*S/S*·*R*” diastereomer possesses an inversion

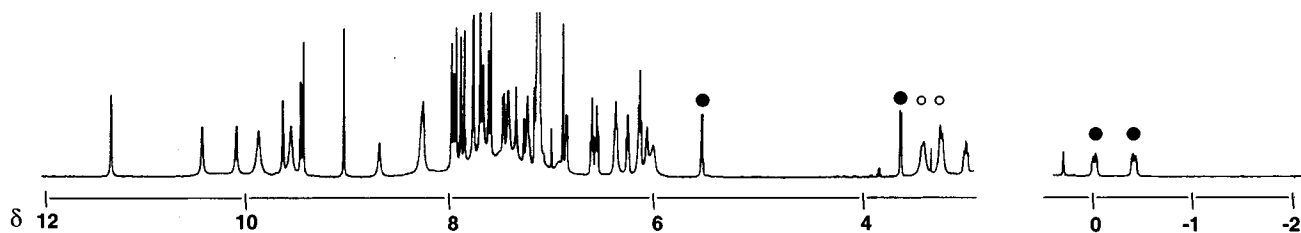


Figure 5. Portions of the ^1H NMR spectrum (600 MHz, benzene- d_6 , 295 K) of cavitand **5**. Signals for the acenaphthene residue are denoted with filled circles (assembled state) and open circles (monomeric state).

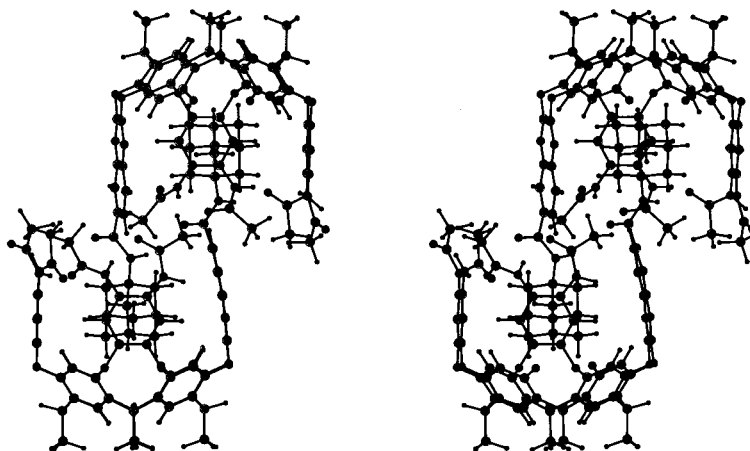


Figure 6. Stereoview of dimer **3a·3a** from the minimized structure obtained using the Amber* force field in MacroModel 6.5. The C_7H_{15} and $\text{C}_{11}\text{H}_{23}$ chains were replaced by CH_3 to expedite the computation. One aromatic wall of each monomeric species was removed (after minimization) for viewing clarity.

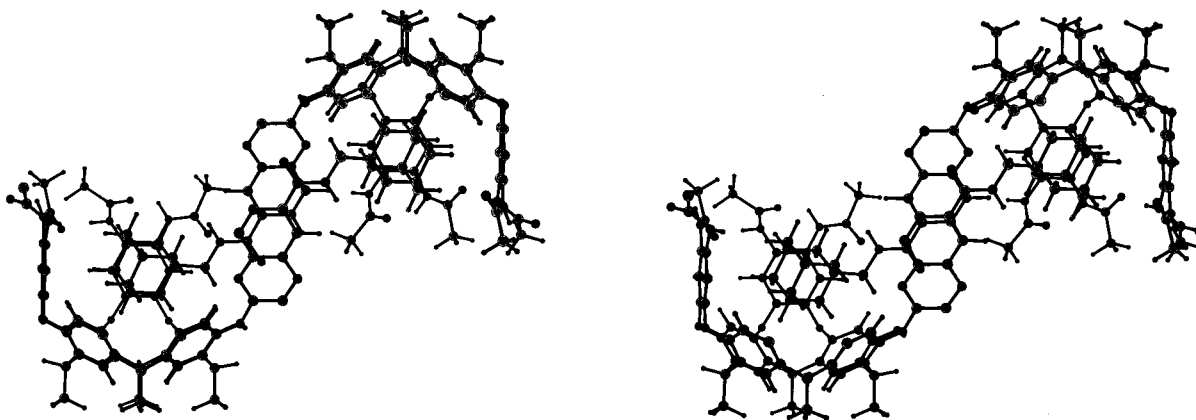


Figure 7. Stereoview of dimer **4b·4b** from the minimized structure obtained using the Amber* force field in MacroModel 6.5. The C_7H_{15} and $\text{C}_{11}\text{H}_{23}$ chains were replaced by CH_3 to expedite the computation. One aromatic wall of each monomeric species was removed (after minimization) for viewing clarity.

center. Hence, a single set of cavitand resonances would be expected for each diastereomeric dimer (i.e., the two halves of each dimer are magnetically equivalent). In fact, the presence of diastereomeric dimers is evident²² in the complex NMR spectra observed for SCCs **3b** and **4b** in *p*-xylene- d_{10} solvent, and moreover, modest diastereoselectivity (ca. 3:1) is apparent in the case of **4b**. Much to our surprise, NMR spectra of dimeric **3a** and **4a** possess a single set of cavitand signals (Figures 2C and 3A). That SCCs **3a** and **4a** should display such a high degree of diastereoselectivity is not readily explained by our modeling studies to date. It is unclear from modeling if the quinoxaline amides participate in hydrogen bonding or if the alkyl groups of the dimer are interdigitated. Lacking structural information of crystallographic detail, we hesitate to speculate at this time

(22) This is supported by the observation of chemical exchange cross-peaks between adamantane signals in the ROESY spectrum of **4b·4b**.

Table 1. Dimerization Constants (K_{dim}) for Self-Complementary Cavitands in Various Solvents at 295 K

	<i>p</i> -xylene- d_{10}	benzene- d_6	CDCl_3
3a	3000 M^{-1}	325 M^{-1}	nd
3b	1800 M^{-1}	50 M^{-1}	nd
10	nd ^a	nd	nd
4a	$\geq 10^5 \text{ M}^{-1}$	-	250 M^{-1}
4b	$\geq 10^5 \text{ M}^{-1}$	-	1000 M^{-1}
4c	50 M^{-1}	-	nd
4d	nd	nd	nd

^a nd = no dimer.

on the identity of the preferred diastereomer or the source of the high diastereoselectivity observed.

Table 1 presents dimerization constants for SCCs **3** and **4** in various solvents. As mentioned previously, the assembly process is highly solvent dependent. Not surprisingly, the best solvents

Table 2. Thermodynamic Parameters for the Dimerization of Self-Complementary Cavitands

cavitand	solvent	ΔH , kcal/mol	ΔS , cal/(mol K)
3a	<i>p</i> -xylene- <i>d</i> ₁₀	-17.2	-41
3b	<i>p</i> -xylene- <i>d</i> ₁₀	-29.9	-85
4a	CDCl ₃	-10.6	-25

for assembly are those that are themselves poor guests. Hence, *p*-xylene-*d*₁₀, a flat aromatic that is a poor match for the nearly cylindrical cavities in **3** and **4**, generally produces the strongest assemblies. Somewhat weaker assemblies are observed in other aromatics such as benzene-*d*₆ and toluene-*d*₈. The roughly spherical CDCl₃ competes well for the cavity. The acidity of its C–D function evidently overcomes the effect of the many nonbonded electrons of the solvent and may also be involved in weakening the intramolecular hydrogen bonds. The upshot is that dimerization is less favored, when it occurs at all. The polar aprotic solvent DMF-*d*₇ is expected to be a good guest for the cavity. Moreover, it can disrupt the hydrogen bonds and thereby compromise the structural integrity of the cavity—no dimerization is observed.

Some other features of the binding cavity and the guest species can be identified (Table 1). Adamantane derivatives are most effective at stabilizing the self-complementary binding motif. The connection between cavitand and adamantane is important with amide linkages being much preferred to esters (compare **4b** and **4c**).²³ Aromatics (e.g., the benzyl ester **10** and **4d**) are no better guests for the cavity than solvent and hence no assembly is observed. Finally, the increased conformational freedom and surface contact present in half-bridged dimers **4-4** produce more stable assemblies than the fully bridged SCCs **3**.

Our experience to date with cavitands **3–5** and related derivatives suggests that their aggregation in solution may be a general phenomena. For example, we were surprised to find that NMR spectra of cavitand **5** contain peculiarities suggestive of an assembled state. As shown in Figure 5, the ¹H NMR spectrum of **5** in benzene-*d*₆ solution possesses a separate set of acenaphthene signals that are shifted upfield by ca. 3 ppm (filled circles, Figure 5). The observation of acenaphthene inclusion cannot be reconciled with a strictly monomeric species, particularly since the intensity of the upfield acenaphthene signals is temperature and concentration dependent. Despite expending considerable experimental effort, we cannot be sure of the specific nature of the aggregation, but it appears not to be a simple symmetrical dimer as is observed with **3** and **4**. We are currently exploring the unusual behavior of cavitand **5** and will report on it more fully in a subsequent report.

Thermodynamics of Assembly. The thermodynamic parameters of assembly in SCCs **3** and **4** were examined using variable-temperature NMR. The slow exchange between monomeric and dimeric species allows concentrations and hence association constants to be easily determined. A van't Hoff plot was then used to derive ΔH and ΔS values for the assembly process. The dimerization was studied using *p*-xylene-*d*₁₀ as solvent whenever possible. In the case of SCC **4**, only dimeric species are observed in *p*-xylene-*d*₁₀ so CDCl₃ solvent was used in this case. The results are summarized in Table 2.

The dimerization of cavitands **3** and **4** is enthalpically favored and entropy opposed. The inclusion of adamantane upon

dimerization is enthalpically favorable due to a multitude of weak binding interactions and a shape complementarity that favors a stronger, more well-organized hydrogen bonding seam (as compared to the solvent-filled monomeric species).

The free energies of dimerization in **3** and **4** are generally small ($\Delta G \approx -2.5$ to -6.7 kcal/mol), but the compensating enthalpic and entropic contributions can be very significant (Table 2). Whereas the open-ended cavitand **2** binds adamantane derivatives with values of $\Delta H = -5.5$ kcal/mol and $\Delta S = -11$ eu, the corresponding values for dimerization of **3** and **4** are between two and six times larger. Since dimerization involves two binding events it might be reasonable to expect ΔH values twice as high (as is the case for dimer **4a·4a**), but what is the source of the additional binding enthalpy for dimer **3·3**? We suggest that interactions between the upper-rim C₇H₁₅ chains in dimer **3·3** may be partially responsible. The more compact structure of dimer **3·3** (as compared to **4·4**) forces several amide C₇H₁₅ chains into close proximity (Figures 6 and 7). To avoid occupying the same space, some of these chains might interdigitate—an entropically costly arrangement that might provide compensating enthalpic benefit²⁴ through a multitude of van der Waals contacts. In contrast, the amide substituents of the more extended dimer **4·4** are free of such interactions and smaller ΔH and ΔS values are observed (Table 2).²⁵ It is interesting to note that the formation of self-included dimer **7·7** (Chart 2) occurs with similarly large enthalpy–entropy compensation ($\Delta H = -21$ kcal/mol, $\Delta S = -58$ eu).¹⁶

Conclusions

Cavitands with self-complementary surfaces (convex and concave) associate in solution to form complexes of high thermodynamic and kinetic stabilities. The cooperation of binding sites in these host–guest hybrids leads to much stronger association than is observed for the component parts alone (adamantane and cavitand). The intermolecular interactions involved are subtle and assembly occurs with significant enthalpy–entropy compensation. Because they are self-complementary structures, a question can be raised as to whether the systems are capable of self-replication. We are currently exploring this possibility and will report on our findings in due course.

Experimental Section

General. Melting points were determined on a Thomas-Hoover capillary melting point apparatus and are uncorrected. ¹H NMR and ¹³C NMR spectra were recorded on Bruker AM-300 and DRX-600 spectrometers. The chemical shifts were measured relative to residual nondeuterated solvent resonances. Matrix-assisted laser desorption/ionization (MALDI) mass spectrometry experiments were performed on a PerSeptive Biosystems Voyager-Elite mass spectrometer with delayed extraction, using 2,5-dihydroxybenzoic acid (DHB) as a matrix. Electrospray ionization (ESI) mass spectra were recorded on an API III Perkin-Elmer SCIEX triple quadrupole mass spectrometer. HRMS values generally agreed to ≤ 5 ppm for compounds with molecular weight ≤ 500 and ≤ 10 ppm for compounds with higher molecular weight ≥ 2000 .²⁶ FTIR spectra were recorded on a Perkin-Elmer Paragon 1000 PC FT-IR spectrometer. Column chromatography was performed with Silica Gel 60 (EM Science or Bodman, 230–400 mesh). All experiments with moisture- or air-sensitive compounds were performed

(24) The source of the increased binding enthalpy and entropy in **3b** (as compared to **3a**) is not readily apparent. Without detailed (crystallographic) information regarding the structure of these dimers, this issue cannot be meaningfully addressed.

(25) This analysis necessarily ignores solvent effects on the thermodynamics of assembly. A direct comparison of SCCs **3** and **4** in the same solvent was not possible due to the strictly dimeric structure of **4** in *p*-xylene-*d*₁₀ solvent.

(23) The surprisingly large effect of this change suggests that the amide plays a crucial role in stabilizing the dimeric structure, probably as a hydrogen bond donor/acceptor. The substitution of amide for ester is destabilizing to a greater extent than simple loss of a hydrogen bond donor and so it seems likely that lone pair–lone pair repulsion is additionally destabilizing in the case of **4c**.

in anhydrous solvents under a nitrogen atmosphere. Compounds **1**,²⁷ 1,2-difluoro-4,5-dinitrobenzene,²⁸ 1,2-diketopyracene,²⁹ and 2,3-dihydroxy-6-quinoxalinecarboxylic acid³⁰ were synthesized in accord with the literature protocols. Molecular modeling was performed using the Amber* force field in the MacroModel 5.5 program.³¹

Hexanitrocavitand 8. Triethylamine (2.23 mL, 16.0 mmol) was added dropwise to a stirred solution of resorcinarene **1** (1.10 g, 1.0 mmol) and 1,2-difluoro-4,5-dinitrobenzene (0.612 g, 3.0 mmol) in anhydrous DMF (50 mL). The resulting mixture was then heated to 70 °C and kept at that temperature for 16 h. The reaction mixture was cooled to room temperature and poured into dilute aqueous HCl (pH ~1, 400 mL). The bright yellow solids were filtered off, washed with large amount of water, and dried in vacuo. Column chromatography (CH₂Cl₂, then 2% MeOH–CH₂Cl₂) provided first the octanitro compound (0.370 g; 0.21 mmol; 21%) and then the desired hexanitro cavitand **8** (0.910 g; 0.57 mmol; 57%) as a yellow solid after trituration with MeOH: mp >250 °C; FTIR (CHCl₃, cm⁻¹) ν 3578, 2919, 2851, 1590, 1543, 1490, 1343, 1286, 1195; ¹H NMR (600 MHz, CDCl₃, 330K) δ 7.63 (s, 2 H), 7.61 (s, 2 H), 7.58 (s, 2 H), 6.95 (s, 2 H), 6.84 (s, 2 H), 6.70 (s, 2 H), 6.60 (s, 2 H), 5.85 (s, 2 H), 4.31 (t, J = 7 Hz, 1 H), 4.00–3.97 (m, 3 H), 2.10–2.01 (m, 8 H), 1.36–1.28 (m, 72 H), 0.90 (t, J = 7 Hz, 12 H); MS-ESI⁻ m/z 1597 ([M – H + ¹³C]⁻ calcd for C₈₉H₁₁₁N₆O₂₀¹³C 1597).

Hexaamide 9. A solution of hexanitro cavitand **8** (3.92 g, 2.45 mmol) in toluene (150 mL) was treated with a catalytic amount of Raney Nickel as a suspension in EtOH (commercial H₂O suspension was pre-washed with EtOH (2 × 5 mL)). The mixture was stirred for 16 h at 40 °C under a H₂ atmosphere. After cooling, the mixture was filtered through a pad of Celite with the aid of MeOH (2 × 50 mL). The filtrates were combined and evaporated under vacuum to give a brown solid (3.52 g) that was protected from air and used directly in the next step. The crude hexaamide was dissolved in 150 mL of degassed (purged with N₂) EtOAc–water (1:1) and K₂CO₃ (4.01 g, 29.4 mmol) was added with vigorous stirring. Octanoyl chloride (2.39 g, 2.50 mL, 14.7 mmol) was added at once, and the resulting mixture was stirred at room temperature for 2 h. The solution was then diluted with half-saturated NaHCO₃ and extracted with EtOAc. The combined organic extracts were washed with brine, dried over MgSO₄, filtered, and concentrated to give 5.40 g of the crude amide. The crude amide product was dissolved in 60 mL of toluene–EtOH (1:1) and treated with hydrazine hydrate (0.613 g, 0.59 mL, 12.3 mmol). The mixture was stirred at 80 °C for 3 h, cooled to room temperature, and concentrated. Column chromatography (0–1% MeOH in CH₂Cl₂) provided the product **9** as a yellow solid after trituration with MeOH (1.44 g, 27% overall): mp >250 °C; FTIR (CHCl₃, cm⁻¹) ν 3684, 3234, 2919, 2852, 1704, 1657, 1600, 1514, 1481, 1404, 1276; ¹H NMR (600 MHz, benzene-*d*₆, 340 K) δ 9.85 (s, 2 H), 9.55 (s, 2 H), 8.70–8.80 (br s, 2 H), 7.74 (s, 2 H), 7.72 (s, 2 H), 7.62 (s, 2 H), 7.60 (s, 2 H), 7.39 (s, 2 H), 7.36 (s, 2 H), 7.07 (s, 2 H), 6.29 (t, J = 8 Hz, 2 H), 6.23 (t, J = 8 Hz, 1 H), 4.73 (t, J = 8 Hz, 1 H), 2.5–1.20 (m, 152 H), 0.94–0.90 (m, 30 H); ¹³C NMR (150 MHz, benzene-*d*₆, 330 K) δ 173.6, 173.4, 173.2, 156.4, 156.1, 155.8, 153.0, 151.3, 151.1, 137.3, 136.9, 132.5, 130.4, 129.5, 124.7, 124.5, 122.4, 121.3, 117.4, 111.7, 38.6, 37.6, 35.5, 34.8, 34.4, 34.3, 34.0, 33.5, 32.7, 32.5, 32.47, 32.4, 30.8, 30.63, 30.6, 30.55, 30.5, 30.3, 30.2, 29.9, 29.86, 29.6, 29.1, 29.0, 27.0, 26.95, 26.3, 23.4, 23.3, 14.6, 14.5; HRMS-MALDI–FTMS m/z 2196.5792 ([M + Na]⁺, calcd for C₁₃₈H₂₀₈N₆O₁₄Na 2196.5645, error 6.7 ppm).

(26) For details on high-resolution mass spectrometry, see: (a) Rose, M. E.; Johnstone, R. A. *Mass Spectrometry for Chemists and Biochemists*; Cambridge University Press: Cambridge, 1982. (b) Jennings, K. R.; Dolnikowski, G. G. *Methods in Enzymology*; McCloskey, J. A., Ed.; Academic Press: New York, 1990; p 37 and references therein.

(27) Tunstad, L. M.; Tucker, J. A.; Dalcanale, E.; Weiser, J.; Bryant, J. A.; Sherman, J. C.; Helgeson, R. C.; Knobler, C. B.; Cram, D. J. *J. Org. Chem.* **1989**, *54*, 1305–1312.

(28) Kazmierczuk, Z.; Dudycz, L.; Stolarski, R.; Shugar, D. *Nucleosides, Nucleotides* **1981**, *8*, 101–117.

(29) Richter, H. J.; Stocker, F. B. *J. Org. Chem.* **1959**, *24*, 366–368.

(30) Kleb, K. G.; Siegel, E.; Sasse, K. *Angew. Chem., Int. Ed.* **1964**, *3*, 408.

(31) Mohamadi, F.; Richards, N. G.; Guida, W. C.; Liskamp, R.; Lipton, M.; Caufield, C.; Chang, G.; Hendrickson, T.; Still, W. C. *J. Comput. Chem.* **1990**, *11*, 440–467.

Benzyl Ester 14. A suspension of 2,3-dihydroxy-6-quinoxaline-carboxylic acid (0.207 g, 1.0 mmol) in SOCl₂ (4 mL) was treated with a catalytic amount of DMF and heated at 80 °C for 3 h. After being cooled to room temperature the clear yellow solution was concentrated to give 2,3-dichloro-6-quinoxalinecarbonyl chloride as a tan solid. This material was then dissolved in 5 mL of CH₂Cl₂ and cooled at 0 °C. The solution was treated with triethylamine (0.404 g, 0.57 mL, 4.0 mmol) and then benzyl alcohol (0.108 g, 0.103 mL, 1.0 mmol) and allowed to warm to room temperature. After being stirred for 16 h, the reaction mixture was poured into a mixture of 10% K₂CO₃ and CH₂Cl₂. The layers were separated and the organic phase washed with brine, dried over MgSO₄, filtered, and concentrated to give ca. 0.30 g of the crude product. Column chromatography (0–20% EtOAc–hexane) provided 0.261 g of **14** as a tan solid: mp 111–112 °C; FTIR (CHCl₃, cm⁻¹) ν 2995, 1719, 1452, 1381, 1295, 1267, 1152, 1119, 1000; ¹H NMR (600 MHz, CDCl₃) δ 8.78 (d, J = 1.4 Hz, 1 H), 8.44 (dd, J = 1.4, 9 Hz, 1 H), 8.10 (d, 9 Hz, 1 H), 7.51–7.35 (m, 5 H), 5.46 (s, 2 H); ¹³C NMR (150 MHz, CDCl₃) δ 164.8, 147.5, 146.6, 142.5, 139.9, 135.3, 132.5, 130.97, 130.7, 128.7, 128.6, 128.5, 128.4, 67.6; HRMS-MALDI-FTMS m/z 333.0194 ([M + H]⁺, calcd for C₁₆H₁₁Cl₂N₂O₂ 333.0198, error 1.2 ppm). Analogously, 2,3-dichloroquinoxalines **13a,b** and **15** were synthesized from 2,3-dichloro-6-quinoxalinecarbonyl chloride and 1-aminoadamantane, 1-aminomethyladamantane, and 1-adamantanol.

General Procedure for the Coupling of Hexaamide 9 with 2,3-Dichloroquinoxalines: Synthesis of Cavitanes 4a–d. An oven-dried 10 mL flask was charged with hexaamide **9** (0.019 g, 0.0087 mmol) and the quinoxaline **13a** (3.6 mg, 0.0096 mmol). The reactants were dissolved in dry DMF (1 mL) and the solution treated with triethylamine (7 μ L, 0.052 mmol). The reaction mixture was heated at 65 °C for 20 h and then allowed to cool to room temperature. The solution was poured into a mixture of EtOAc (10 mL) and dilute aqueous HCl (10 mL). The layers were separated and the aqueous phase extracted with two 10 mL portions of ethyl acetate. The combined organic extracts were washed with brine, dried over Na₂SO₄, filtered, and concentrated to provide 0.024 g of the crude product. Column chromatography (0–20% EtOAc–hexane) provided 9 mg (42%) of cavitand **4a** as a pale yellow oil: FTIR (CHCl₃, cm⁻¹) ν 3244, 3014, 2918, 2852, 1657, 1514, 1481, 1400, 1324, 1276, 895 cm⁻¹; ¹H NMR (Figure 3A, 600 MHz, *p*-xylene-*d*₁₀) δ 10.3 (s, 1 H), 9.87 (s, 1H), 9.85 (s, 1 H), 9.79 (s, 1 H), 9.68 (s, 1 H), 9.54 (s, 1 H), 8.9 (s, 2 H), 8.05–7.15 (12 s, 15 H), 6.35–6.25 (m, 4 H), 6.01 (s, 1H), 5.90 (br tr, 1 H), 3.1–1.1 (m, 152 H), 1.0–0.8 (m, 30 H), 0.8–0.7 (m, 6 H), –0.58 (s, 3 H), –0.83 (d, J = 11 Hz, 3 H), –1.07 (d, J = 11 Hz, 3 H); MALDI-MS m/z 2536 ([M + Na]⁺ calcd for C₁₅₇H₂₂₆ClN₉O₁₅Na 2536).

Cavitand 4b: 11 mg of pale yellow oil, 51%; FTIR (CHCl₃, cm⁻¹) ν 3244, 3014, 2928, 2852, 1657, 1510, 1481, 1405, 1271, 890 cm⁻¹; ¹H NMR (Figure 3B, 600 MHz, *p*-xylene-*d*₁₀) δ 10.75 (s, 1 H, minor diastereomer), 10.1–9.4 (9 s, 5 H, both diastereomers), 9.1–8.8 (3 s, 2 H, both), 8.4–7.0 (14 s, 17 H, both), 6.4–6.3 (m, 4 H, both), 5.9 (s, 1H, major diastereomer), 5.7 (s, 1 H, minor), 2.9–1.1 (m, 154 H), 1.1–0.8 (m, 30 H), 0 to –0.6 (m, 15 H); MALDI MS m/z 2551 ([M + Na]⁺ calcd for C₁₅₈H₂₂₈ClN₉O₁₅Na 2550).

Cavitand 4c: 13 mg of pale yellow oil, 65%; FTIR (CHCl₃, cm⁻¹) ν 3407, 3244, 2919, 2851, 1714, 1662, 1600, 1509, 1481, 1405, 1267, 1195; ¹H NMR (600 MHz, CDCl₃) δ 9.56 (s, 1 H), 9.47 (s, 1 H), 9.37 (s, 1 H), 9.15 (s, 1 H), 8.72 (s, 1 H), 8.24 (d, J = 9 Hz, 1 H), 8.1 (s, 1 H), 7.73 (s, 1 H), 7.63 (d, J = 9 Hz, 1 H), 7.51–7.06 (8 s, 12 H), 6.70 (s, 1 H), 6.50 (s, 1 H), 5.86 (t, J = 8 Hz, 1 H), 5.83 (t, J = 8 Hz, 1 H), 5.73 (t, J = 8 Hz, 1 H), 4.25 (t, J = 8 Hz, 1 H), 3.99 (dd, J = 5 Hz, 5 Hz, 2 H), 2.5–1.0 (m, 167 H), 1.0–0.8 (m, 30 H); MALDI MS m/z 2552 ([M + Na]⁺ calcd for C₁₅₈H₂₂₇ClN₉O₁₆Na 2551).

Cavitand 4d: 0.104 g of pale yellow oil, 55%; FTIR (CHCl₃, cm⁻¹) ν 3407, 3244, 2928, 2852, 1719, 1657, 1514, 1486, 1404, 1267; ¹H NMR (600 MHz, CDCl₃) δ 9.62 (s, 1 H), 9.54 (s, 1 H), 9.32 (s, 1 H), 9.13 (s, 1 H), 8.76 (s, 1 H), 8.24 (d, J = 9 Hz, 1 H), 7.79 (s, 1 H), 7.69 (s, 1 H), 7.60 (d, J = 9 Hz, 1 H), 7.50–7.04 (8 s, 18 H), 6.85 (s, 1 H), 6.70 (s, 1 H), 5.85 (t, J = 8 Hz, 1 H), 5.82 (t, J = 8 Hz, 1 H), 5.71 (t, J = 8 Hz, 1 H), 5.42 (dd, J = 8 Hz, 2 Hz, 2 H), 4.27 (t, J = 8 Hz, 1 H), 2.5–1.0 (m, 152 H), 1.0–0.8 (m, 30 H); MALDI MS m/z 2509 ([M + K]⁺ calcd for C₁₅₄H₂₁₇ClN₈O₁₆K 2509).

Benzyl Ester 10. An oven-dried 10 mL flask was charged with hexaamide **9** (0.103 g, 0.047 mmol) and the quinoxaline **14** (17.3 mg, 0.052 mmol). The reactants were dissolved in dry DMF (4 mL) and the solution treated with triethylamine (39 μ L, 0.282 mmol). The reaction mixture was heated at 85 °C for 48 h and then allowed to cool to room temperature. The solution was poured into a mixture of EtOAc (20 mL) and dilute aqueous HCl (20 mL). The layers were separated and the aqueous phase extracted with two 20 mL portions of EtOAc. The combined organic extracts were washed with brine, dried over MgSO₄, filtered, and concentrated to provide the crude product. Column chromatography (0–20% ethyl acetate–hexane) provided 59 mg (55%) of cavitand **10** as a pale yellow oil: FTIR (CHCl₃, cm⁻¹) ν 3416, 3244, 2919, 2852, 1662, 1600, 1514, 1481, 1400, 1267, 1195; ¹H NMR (600 MHz, CDCl₃) δ 9.53 (s, 1 H), 9.43 (s, 1 H), 9.18 (s, 1 H), 8.52 (s, 2 H), 8.37 (d, J = 8 Hz, 1 H), 8.3 (br s, 1 H), 8.02 (d, J = 8 Hz, 1 H), 7.78 (s, 1 H), 7.74 (s, 2 H), 7.72 (s, 1 H), 7.66 (s, 1 H), 7.45–7.37 (m, 7 H), 7.28 (s, 1 H), 7.26 (s, 2 H), 7.24 (s, 1 H), 7.20 (s, 2 H), 7.19 (s, 2 H), 5.80 (t, J = 8 Hz, 1 H), 5.75 (t, J = 8 Hz, 2 H), 5.50 (t, J = 8 Hz, 1 H), 5.42 (d, J = 12 Hz, 1 H), 5.33 (d, J = 12 Hz, 1 H), 2.5–1.0 (m, 152 H), 1.0–0.8 (m, 30 H); MALDI MS m/z 2556 ([M + Na]⁺ calcd for C₁₅₄H₂₂₇N₉O₁₅Na¹³C 2556.6).

Pentafluorophenyl Ester 12. To a solution of benzyl ester **10** (0.059 g, 0.025 mmol) in EtOAc (4 mL) was added 0.059 g of Pd/C. The suspension was stirred under a H₂ atmosphere for 2 h and then filtered through Celite twice. The filtrate was concentrated to give 0.046 g of the acid **11** which was converted directly to **12** without further purification. The crude acid **11** (0.046 g, 0.020 mmol) was dissolved in 3 mL of THF and treated with EDC–MeI (0.012 g, 0.040 mmol), pentafluorophenol (4.0 mg, 0.022 mmol), and (dimethylamino)pyridine (0.6 mg, 0.005 mmol). The suspension was sonicated briefly and then stirred in the dark for 20 h. The reaction mixture was then passed through a small column eluting with THF. The fractions containing product were collected and concentrated to provide 0.050 g (78% overall) of active ester **12** as a yellow film: FTIR (CHCl₃, cm⁻¹) ν 3416, 3244, 2919, 2852, 1757, 1657, 1519, 1481, 1400, 1338, 1190; ¹H NMR (600 MHz, CDCl₃, 295 K) δ 9.44 (s, 1 H), 9.36 (s, 1 H), 9.27 (s, 1 H), 9.05 (s, 1 H), 8.9 (s, 1 H), 8.78 (s, 1 H), 8.44 (s, 1 H), 8.20 (d, J = 8 Hz, 1 H), 8.1–7.2 (m, 15 H), 5.8–5.75 (m, 3 H), 5.45 (br t, 1 H), 2.6–1.0 (m, 152 H), 1.0–0.8 (m, 30 H); ¹⁹F NMR (565 MHz, CDCl₃) δ -151.8 (d, J = 20 Hz, 2 F), -156.5 (t, J = 20 Hz, 1 F), -161.5 (t, J = 20 Hz, 2 F).

Self-Complementary Cavitand 3a. A 10 mL oven-dried flask was charged with active ester **12** (13.3 mg, 0.0052 mmol) and 1-aminoadamantane (1.0 mg, 0.0066 mmol) in DMF (0.5 mL). The solution was treated with triethylamine (2.0 mg, 3.0 μ L, 0.021 mmol) and stirred at room temperature for 16 h. The solution was then poured into a mixture of EtOAc (10 mL) and dilute HCl (10 mL). The layers were separated and the aqueous phase extracted with two 10 mL portions of EtOAc. The combined organic extracts were washed with brine, dried over Na₂SO₄, filtered, and concentrated to provide 0.013 g of the crude product. Column chromatography (0–20% EtOAc–hexane) provided 10.2 mg (79%) of the cavitand **3a** as a pale yellow oil: FTIR (CHCl₃, cm⁻¹) ν 3684, 3244, 2919, 2852, 1657, 1600, 1514, 1481, 1405, 1229; ¹H NMR (600 MHz, CDCl₃) δ 9.65 (s, 1 H), 9.54 (s, 1 H), 9.44 (s, 1 H), 9.12 (s, 1 H), 8.68 (s, 1 H), 8.47 (d, J = 8 Hz, 1 H), 8.15 (s, 1 H), 8.04 (s, 1 H), 7.95 (s, 1 H), 7.82 (s, 1 H), 7.76–7.73 (3 s, 3 H), 7.60 (s, 1 H), 7.39 (d, J = 8 Hz, 1 H), 7.21–7.10 (4 s, 8 H), 5.90 (s, 1 H), 5.81 (t, J = 8 Hz, 1 H), 5.73 (m, 2 H), 5.59 (t, J = 8 Hz, 1 H), 2.70 (br t, 2 H), 2.5–1.0 (m, 165 H), 1.0–0.8 (m, 30 H); MALDI–FTMS m/z 2500.7060 ([M + Na]⁺ calcd for C₁₅₆H₂₂₅N₉O₁₅Na¹³C 2500.7051, error 0.4 ppm).

Self-Complementary Cavitand 3b. A 10 mL oven-dried flask was charged with active ester **12** (12 mg, 0.0048 mmol) and 1-amino-methyladamantane (1.0 mg, 0.0062 mmol) in CH₂Cl₂ (0.5 mL). The solution was treated with triethylamine (1.9 mg, 2.7 μ L, 0.019 mmol) and stirred at room temperature for 24 h. The reaction mixture was then concentrated and the residue purified by column chromatography (0–20% EtOAc–hexane) to provide 8.2 mg (70%) of the cavitand **3b** as a pale yellow oil: FTIR (CHCl₃, cm⁻¹) ν 3684, 3234, 2919, 2852, 1657, 1600, 1510, 1481, 1405, 1338, 1271; ¹H NMR (600 MHz, CDCl₃, 320 K) δ 9.40 (s, 1 H), 9.31 (s, 1 H), 9.20 (s, 1 H), 8.90 (s, 1 H), 8.40

(s, 1 H), 8.32 (s, 1 H), 8.21 (s, 2 H), 7.91 (s, 1 H), 7.79 (s, 2 H), 7.78 (s, 1 H), 7.64 (s, 2 H), 7.56 (s, 1 H), 7.30–7.28 (3 s, 4 H), 7.25 (s, 1 H), 7.24 (s, 1 H), 7.20 (s, 1 H), 7.18 (s, 1 H), 6.45 (s, 1 H), 5.82–5.75 (m, 3 H), 5.66 (t, J = 8 Hz, 1 H), 3.3 (m, 1 H), 3.0 (m, 1 H), 2.5–1.0 (m, 167 H), 1.0–0.8 (m, 30 H); MALDI–FTMS m/z 2514.7289 ([M + Na]⁺ calcd for C₁₅₇H₂₂₇N₉O₁₅Na¹³C 2514.7208, error 3.2 ppm).

Dinitrocavitand 16. A solution of hexaamide **9** (0.135 g, 0.062 mmol), 1,2-difluoro-4,5-dinitrobenzene (0.025 g, 0.124 mmol), and triethylamine (0.070 mL; 0.5 mmol) in anhydrous DMF (18 mL) was stirred for 14 h at 70 °C. The reaction mixture was then poured into dilute aqueous HCl (pH ~1, 150 mL) and the resulting precipitate was filtered and rinsed with water. After being dried in vacuo, the solids were chromatographed (10% EtOAc–hexane). The product was obtained as a yellow solid after trituration with MeOH (124 mg, 0.053 mmol, 85%); mp >250 °C; ¹H NMR (600 MHz, benzene-*d*₆, 295 K) δ 9.79 (s, 2 H), 9.74 (s, 2 H), 8.53 (br s, 2 H), 7.75 (s, 4 H), 7.67 (s, 4 H), 7.56 (br s, 2 H), 7.45 (br s, 2 H), 7.34 (br s, 2 H), 7.28 (s, 2 H), 6.38 (t, J = 8 Hz, 2 H), 6.15 (t, J = 8 Hz, 1 H), 5.93 (t, J = 8 Hz, 1 H), 2.56–2.37 (m, 20 H), 1.87–1.83 (m, 12 H), 1.55–1.28 (m, 120 H), 0.97–0.89 (m, 30 H); MALDI–MS m/z 2361 ([M + Na]⁺ calcd for C₁₄₄H₂₀₈N₈O₁₈Na 2362).

Diamino Cavitand 17. Dinitrocavitand **16** (0.124 g, 0.053 mmol) was dissolved in toluene (40 mL). To this solution was added a catalytic amount of Raney Nickel that had been previously washed with MeOH (2 \times 5 mL). The resulting suspension was stirred for 3 h at 40 °C under a H₂ atmosphere. After cooling, the Raney Nickel was decanted and the supernatant liquid was pipetted off, rinsing the residual nickel with MeOH (2 \times 10 mL). The filtrates were combined and evaporated under vacuum to give a yellowish solid (0.079 g, 0.0347 mmol, 65%) that was used in the next step without further purification: ¹H NMR (600 MHz, benzene-*d*₆, 295 K) δ 10.00 (s, 2 H), 9.52 (s, 2 H), 9.05 (s, 2 H), 7.77 (s, 2 H), 7.75 (s, 2 H), 7.59 (s, 4 H), 7.50 (s, 2 H), 7.43 (s, 2 H), 7.36 (s, 2 H), 6.95 (s, 2 H), 6.41 (t, J = 8 Hz, 1 H), 6.34 (t, J = 8 Hz, 1 H), 6.27 (t, J = 8 Hz, 2 H), 3.28 (br, 4 H), 2.46–2.22 (m, 20 H), 1.88–1.65 (m, 12 H), 1.54–1.25 (m, 120 H), 0.98–0.92 (m, 30 H); MALDI–MS m/z 2279 ([M + H]⁺ calcd for C₁₄₄H₂₁₂N₈O₁₄H 2278.6).

Cavitand 5. To a stirred solution of diamine **17** (0.024 g, 0.0105 mmol) and 1,2-diketopyracene (7 mg, 0.032 mmol) in THF (5 mL) was added glacial acetic acid (30 μ L) and the resulting mixture was refluxed for 16 h.³² After cooling, the volatiles were removed under vacuum and the residue was purified by preparative thin-layer chromatography (silica gel, 0.5 mm) eluting with 20% EtOAc–hexane. The product was obtained as a yellow solid (13 mg, 0.0053 mmol, 50%) after trituration with MeOH: mp >250 °C; FTIR (CDCl₃, cm⁻¹) ν 3238, 3034, 2957, 2928, 2855, 1968, 1731, 1658, 1600, 1511, 1482, 1436, 1273, 1189, 1058, 850; ¹H NMR (600 MHz, CDCl₃, 340 K) δ 9.25 (br, 4 H), 8.46 (br, 4 H), 7.68 (br, 4 H), 7.47 (br, 6 H), 7.32 (s, 2 H), 7.29 (s, 2 H), 7.22 (s, 2 H), 5.84–5.79 (m, 3 H), 5.64 (br, 1 H), 3.67 (dd, J = 17.3, 22.2 Hz, 4 H), 2.50–2.02 (m, 20 H), 1.80–1.25 (m, 132 H), 0.93–0.84 (m, 30 H); ¹³C NMR (150 MHz, CDCl₃, 295 K) δ 172.88, 172.45, 172.40, 163.10, 162.74, 155.04, 154.76, 154.46, 154.21, 153.56, 149.66, 149.40, 136.67, 135.90, 135.50, 135.35, 134.95, 128.97, 127.94, 127.79, 127.62, 124.35, 123.72, 123.48, 122.05, 121.21, 120.82, 116.22, 37.22, 33.79, 33.35, 33.30, 32.83, 32.66, 32.25, 31.95, 31.72, 31.64, 29.83, 29.82, 29.78, 29.73, 29.42, 29.36, 29.25, 29.08, 28.99, 28.05, 26.08, 25.80, 22.70, 22.55, 14.13, 14.06, 13.99; MALDI–MS m/z 2453 ([M + H]⁺ calcd for C₁₅₈H₂₁₆N₈O₁₄H 2452.5); HRMS–MALDI–FTMS m/z 2473.6491 ([M + Na]⁺ calcd for C₁₅₇H₂₁₆N₈O₁₄Na¹³C 2473.6367, error 5.0 ppm).

Acknowledgment. We are grateful to the Skaggs Foundation, the NASA Astrobiology Institute, and the National Institutes of Health for support of this work. We also thank Prof. T. Haino for experimental advice.

JA993922E

(32) This synthetic approach was employed in the synthesis of deepened cavitands: Tucci, F. C.; Rudkevich, D. M.; Rebek, J., Jr. *J. Org. Chem.* **1999**, *64*, 4555–4559.